Multiplanar Sinus CT: A Systematic Approach to Imaging Before Functional Endoscopic Sinus Surgery

Jenny K. Hoang[1]
James D. Eastwood[1]
Christopher L. Tebbit[2]
Christine M. Glastonbury[3]

OBJECTIVE. The purpose of this essay is to present a systematic approach to the use of coronal, axial, and sagittal images for CT evaluation of the sinuses before functional endoscopic sinus surgery (FESS).

CONCLUSION. We present a systematic approach to the use of coronal, axial, and sagittal images in CT evaluation before FESS. Each imaging plane is valuable for displaying anatomic variants, which can predispose a patient to recurrent disease and affect the surgical approach, and critical variants, which can make surgery hazardous.

The aim of functional endoscopic sinus surgery (FESS) to improve mucociliary clearance of the sinuses by removing diseased mucosa and bone that obstruct the sinus outflow tracts. During CT in preparation for FESS, the radiologist looks for anatomic variants, which can predispose the patient to recurrent disease and affect operative technique, and for critical variants, which make surgery hazardous. We present a systematic approach to the use of coronal, axial, and sagittal images in CT evaluations before FESS (Fig. 1).

FESS Technique and Complications

The aim of FESS is to preserve mucosa while restoring drainage and ventilation of the sinuses. Figure 2 shows the steps of the FESS technique. Figure 3 shows the CT appearance after FESS. After the ostiomeatal complex is accessed through the nostril with a rigid endoscope, the ostia and recesses are targeted, depending on the location and pattern of disease. Operations on the frontal sinus alone can be performed if ethmoidectomy does not improve frontal sinus drainage [1]. The posterior ethmoidal and sphenoidal sinuses usually are accessed through the anterior ethmoidal air cells. Preoperative CT also can provide data for intraoperative stereotactic guidance systems, which are used to manage complex disease, and for revision surgery. The incidence of major complications of FESS is 0.4–1.3% [2–4]. Major complications include damage to the optic nerve, CSF leak, meningitis, carotid vascular injury, orbital hematoma, and nasolacrimal duct stenosis.

CT Imaging Technique

At our institutions, axial CT images of the sinuses are acquired with 0.625-mm collimation. From the raw data, we reformat coronal, axial, and sagittal 2.5-mm-thick contiguous images with bone and soft-tissue algorithms.

CT Assessment of Sinuses Before FESS

The radiologist's role is to report on five key points: the extent of sinus opacification, opacification of sinus drainage pathways, anatomic variants, critical variants, and condition of soft tissues of the brain, neck, and orbits. These goals can be covered with a systematic approach to CT in the coronal, axial, and sagittal planes.

Sinus Disease

A description of sinus disease should include the pattern and location; presence of mucosal thickening, opacification, or mass; and associated bone changes of erosion, sclerosis, or sinus expansion. High-attenuation opacification usually represents viscous or desiccated secretions but also raises the possibility of coexisting noninvasive fungal infection (Fig. 4). This diagnosis alters surgical technique because treatment requires thorough removal of fungal debris.

The radiologist should search carefully for potential causes and complications of sinus disease, such as an obstructing tumor and spread of infection to the orbits, brain, or bone (Fig. 5). Mimics of sinus disease, such as tumors and cephaloceles, should be considered when adjacent bone dehiscence is found (Figs. 6 and 7).

Keywords: complications, CT, FESS, functional endoscopic sinus surgery, preoperative

DOI:10.2214/AJR.09.3584

Received September 4, 2009; accepted after revision December 1, 2009.

[1]Department of Radiology, Division of Neuroradiology, Duke University Medical Center, Box 3808, Erwin Rd., Durham NC, 27710. Address correspondence to J. K. Hoang.

[2]Department of Otolaryngology, Charlotte Eye Ear Nose and Throat Associates, Belmont, NC.

[3]Department of Radiology, Division of Neuroradiology, University of California, San Francisco, San Francisco, CA.

CME
This article is available for CME credit.
See www.arrs.org for more information.

WEB
This is a Web exclusive article.

AJR 2010; 194:W527–W536

0361–803X/10/1946–W527

Sinus Drainage Pathways

Evaluating the patency of sinus drainage pathways is crucial because these ostia and recesses are targets during FESS. CT in the coronal plane best shows the ostiomeatal complex and correlates with endoscopy (Figs. 1A and 2). The ostiomeatal complex is the most common site of inflammatory disease and serves as the final drainage pathway for the maxillary, anterior ethmoidal, and frontal sinuses to the middle meatus. The axial plane is valuable for identifying the basal lamella, which divides the anterior and posterior ethmoidal sinuses (Fig. 1B). The sphenoidal ostia and sphenoethmoidal recess are also well depicted on axial images. Use of the often less-used sagittal plane allows excellent evaluation of the frontal recess and frontal sinus drainage pathway (Fig. 1E) [1]. Sagittal images also display the drainage of anterior ethmoidal air cells into the middle meatus and posterior ethmoidal air cells into the sphenoethmoidal recess (Fig. 1D).

Anatomic Variants

A large number of anatomic variants can narrow the sinus drainage pathways and limit surgical access [5].

Nasal septum variants—Nasal septal deflections and spurs are best visualized in the coronal plane (Fig. 3A). Reporting the direction of septal deviation is helpful for surgical planning because the patient may need septoplasty at the beginning of FESS (Fig. 3B). Similarly, nasal turbinate reduction may be performed for an obstructing edematous inferior nasal turbinate (Fig. 8).

Ostiomeatal complex variants—Concha bullosa may not be appreciated through the endoscope when the turbinate is covered by mucosa (Fig. 2A) [6]. In rare instances, concha bullosa is complicated by a polyp, cyst, pyocele, or mucocele (Fig. 5) [7]. Another important variant is lateral deviation of the uncinate process, which can increase the risk of medial orbital wall injury during uncinectomy.

Frontal recess variants—Anatomic variants of the frontal recess are best appreciated on sagittal images. The frontal recess can be narrowed by enlargement of the bordering agger nasi cell and ethmoidal bulla or the presence of variant anterior ethmoidal air cells in the frontal recess. Failure to resect these cells during frontal sinus endoscopic surgery can lead to recurrent disease [5].

Critical Variants

Critical variants are best appreciated on coronal images.

Cribriform plate—The lateral lamella is the thinnest part of the cribriform plate and at risk of fracture during FESS, especially when the olfactory fossae are deep or asymmetric (Fig. 9). The depth of the olfactory fossa can be graded with the Keros classification (Fig. 9) [8]. Fractures of the cribriform plate (Fig. 10) can cause dura mater and bone defects that lead to the early complication of ascending meningitis and the late complication of intracranial hypotension from CSF leak, meningocele, or meningoencephalocele.

Lamina papyracea—Congenital or posttraumatic dehiscence of the lamina papyracea can provide a direct route for sinus surgery instruments to cause orbital injury (Fig. 4). The most common injuries are medial rectus muscle laceration, orbital hematoma, and orbital fibrosis [9]. The anterior ethmoidal artery courses through a bone canal in the superior lamina papyracea and serves as a surgical landmark (Fig. 11). When it courses below the skull base through the ethmoidal air cells, the artery can be inadvertently injured. Retraction of a severed artery into the orbit can cause an orbital hematoma, which requires urgent decompression.

Sphenoidal sinus—Focal bone dehiscence of the sphenoidal sinus places the adjacent optic nerve, internal carotid artery, and trigeminal nerve at risk of injury by surgical instruments (Fig. 4). The optic nerve also may be at risk when Onodi cells, which are posterior ethmoidal air cell variants of sphenoethmoidal air cells, are present (Fig. 12).

Soft Tissues

Images obtained with soft-tissue windows can be used to detect extrasinus extension of disease and incidental brain, orbit, and neck lesions. These pathologic findings can mimic signs of sinus disease and may require further management.

Conclusion

Radiologists should be familiar with the FESS technique and have a systematic approach to reviewing sinus CT scans for sinus disease, drainage pathways, anatomic variants, critical variants, and soft tissues of the brain, neck, and orbits.

References

1. Huang BY, Lloyd KM, DelGaudio JM, Jablonowski E, Hudgins PA. Failed endoscopic sinus surgery: spectrum of CT findings in the frontal recess. *RadioGraphics* 2009; 29:177–195
2. Cumberworth VL, Sudderick RM, Mackay IS. Major complications of functional endoscopic sinus surgery. *Clin Otolaryngol Allied Sci* 1994; 19:248–253
3. Dessi P, Castro F, Triglia JM, Zanaret M, Cannoni M. Major complications of sinus surgery: a review of 1192 procedures. *J Laryngol Otol* 1994; 108:212–215
4. Nguyen QA, Cua DJ, Ng M, Rice DH. Safety of endoscopic sinus surgery in a residency training program. *Ear Nose Throat J* 1999; 78:898–902, 904
5. Earwaker J. Anatomic variants in sinonasal CT. *RadioGraphics* 1993; 13:381–415
6. Bolger WE, Butzin CA, Parsons DS. Paranasal sinus bony anatomic variations and mucosal abnormalities: CT analysis for endoscopic sinus surgery. *Laryngoscope* 1991; 101:56–64
7. Laine FJ, Smoker WR. The ostiomeatal unit and endoscopic surgery: anatomy, variations, and imaging findings in inflammatory diseases. *AJR* 1992; 159:849–857
8. Keros P. Uber die praktische Bedeutung der Niveauunterschiede der Lamina cribrosa des Ethmoids. *Z Laryngol Rhinol Otol* 1962; 41:808–813
9. Bhatti MT, Schmalfuss IM, Mancuso AA. Orbital complications of functional endoscopic sinus surgery: MR and CT findings. *Clin Radiol* 2005; 60:894–904

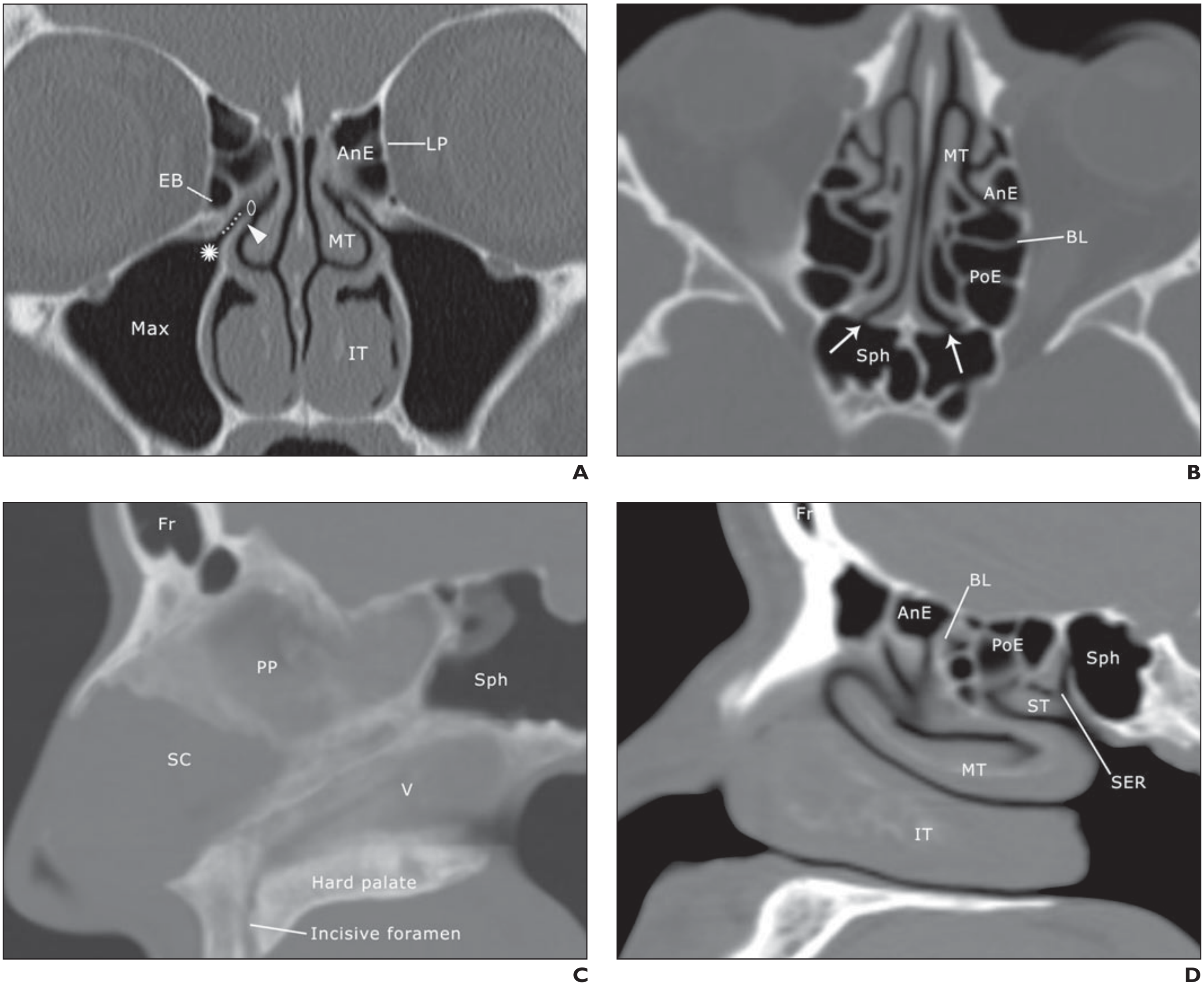

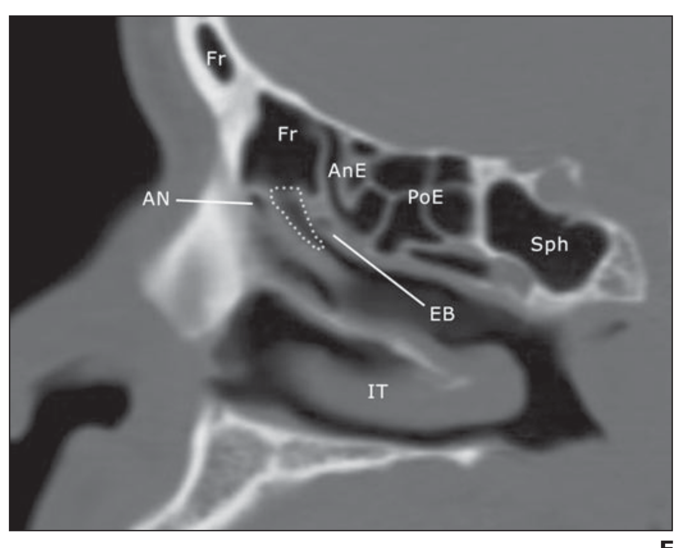

Fig. 1—34-year-old woman with normal sinus anatomy.
A, Coronal CT image shows ostiomeatal complex, which consists of four structures: hiatus semilunaris (*oval*), uncinate process (*arrowhead*), infundibulum (*dotted line*), ethmoidal bulla (EB), and maxillary ostium (*asterisk*). Max = maxillary sinus, IT = inferior turbinate, MT = middle turbinate, AnE = anterior ethmoidal air cells, LP = lamina papyracea.
B, Axial CT image through sphenoidal sinus (Sph), sphenoidal ostia (*arrows*), and ethmoidal air cells shows basal lamella (BL) is lateral attachment of middle turbinate (MT) to lamina papyracea and is division between anterior (AnE) and posterior (PoE) ethmoidal air cells.
C, Midline sagittal CT image shows nasal septum, which is composed of perpendicular plate (PP) of cribriform bone, vomer (V), and septal cartilage (SC). Fr = frontal sinus, Sph = sphenoidal sinus.
D, Sagittal CT image shows sphenoethmoidal recess (SER) and basal lamella (BL) of medial turbinate (MT). Fr = frontal sinus, AnE = anterior ethmoidal air cells, PoE = posterior ethmoidal air cells, ST = superior turbinate, Sph = sphenoidal sinus, IT = inferior turbinate.
E, Sagittal CT image shows frontal recess (*dotted line*), which is bordered by agger nasi cell (AN) and ethmoidal bulla (EB). Fr = frontal sinus, AnE = anterior ethmoidal air cells, PoE = posterior ethmoidal air cells, Sph = sphenoidal sinus, IT = inferior turbinate.

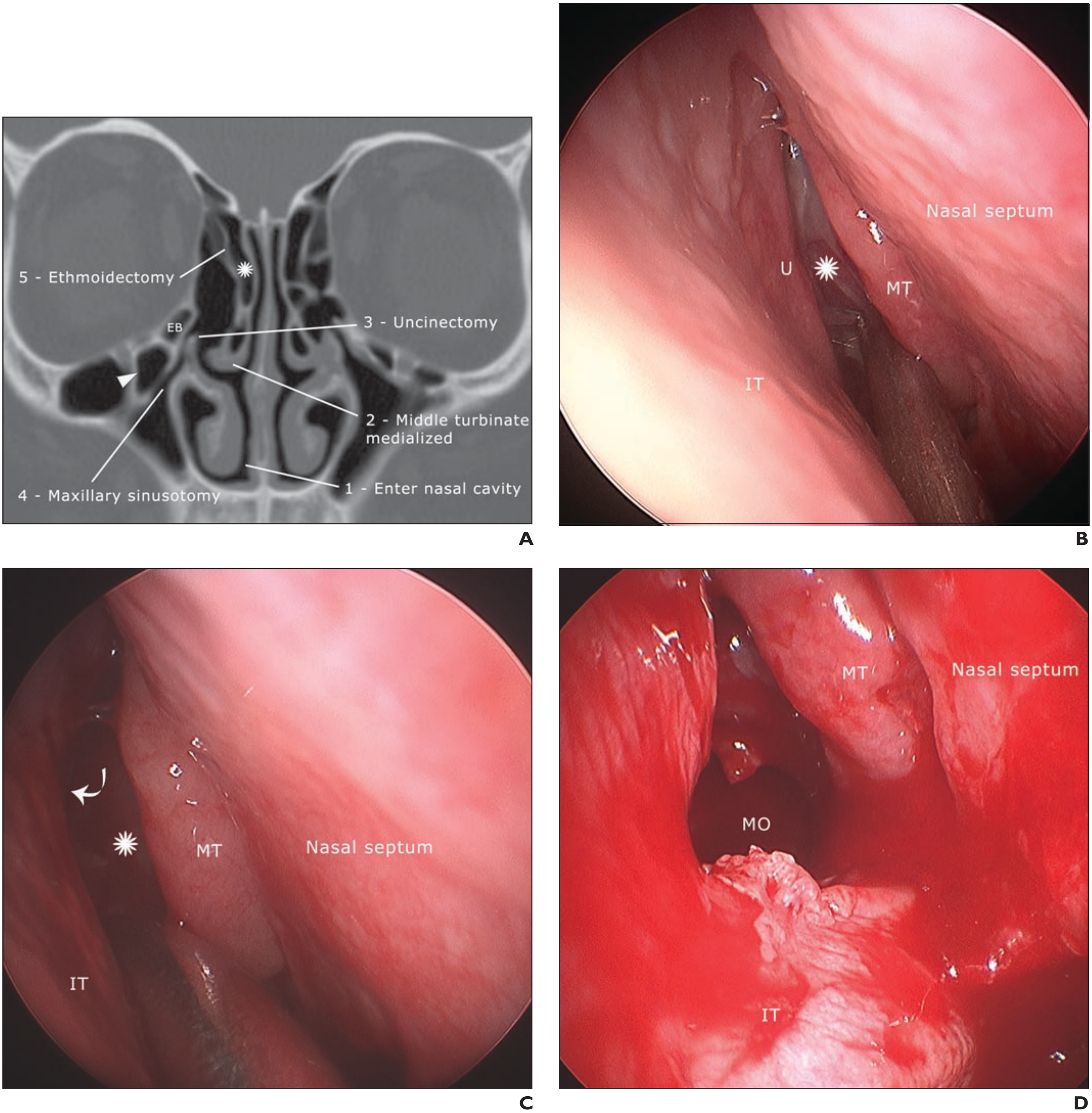

Fig. 2—65-year-old man undergoing functional endoscopic sinus surgery.
A, Labeled coronal CT image shows stages of procedure and anatomic variants of large right Haller cell (*arrowhead*), small left Haller cells, bilateral concha bullosa, and right concha lamella (*asterisk*). EB = ethmoidal bulla.
B, Endoscopic image of right nasal cavity shows inferior turbinate (IT), nasal septum, medialized middle turbinate (MT), and uncinate process (U). Hiatus semilunaris (*asterisk*) contains purulent material.
C, Endoscopic image shows right nasal cavity after uncinectomy with increased exposure of ostiomeatal complex, including maxillary ostium (*arrow*). Asterisk indicates hiatus semilunaris. IT = inferior turbinate, MT = middle turbinate.
D, Endoscopic image shows maxillary ostium (MO) after sinusotomy. MT = middle turbinate, IT = inferior turbinate.

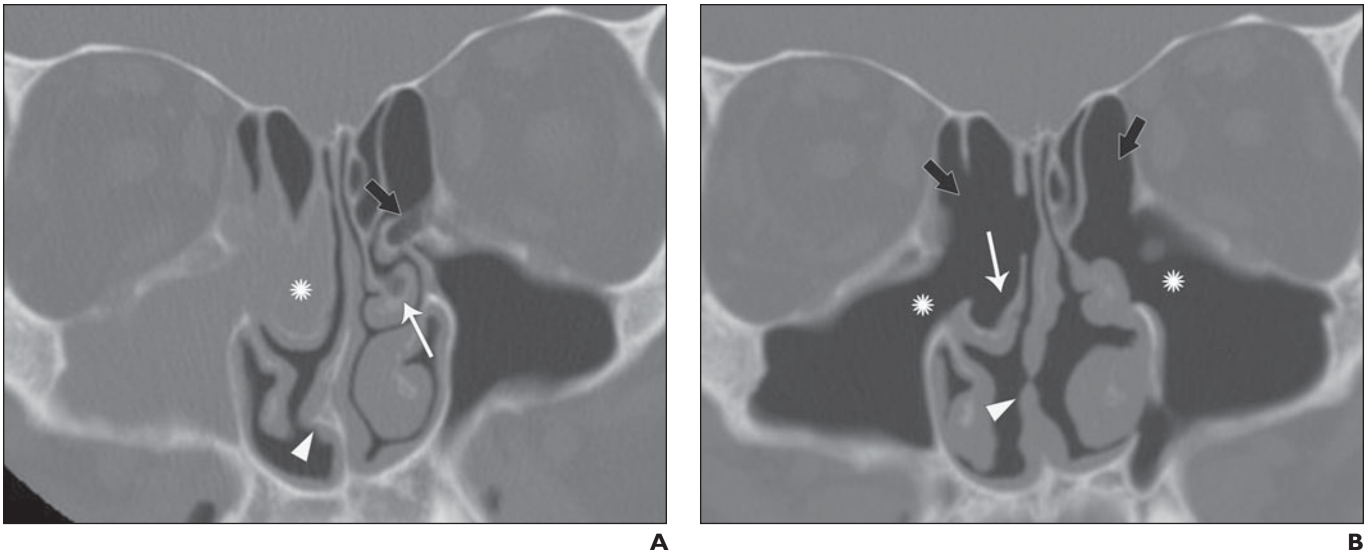

Fig. 3—50-year-old man with chronic sinusitis managed with functional endoscopic sinus surgery (FESS).
A, Coronal CT image obtained before FESS shows complete opacification of right maxillary sinus and partial opacification of right ethmoidal sinus. Right ostiomeatal complex is obstructed. Large opacified right concha bullosa (*asterisk*) and small unopacified left concha bullosa (*white arrow*) are evident. Left ethmoidal bulla (*black arrow*) is large and abuts left uncinate process. Nasal septum is deviated to right with right nasal spur (*arrowhead*).
B, Coronal CT image obtained 2 months after FESS shows resolution of mucosal disease of right sinus. Signs of surgery are septoplasty (*arrowhead*), bilateral uncinectomy, and bilateral maxillary sinusotomies (*asterisks*). Resection of right concha bullosa (*white arrow*) and bilateral ethmoidectomy (*black arrows*) also have been performed.

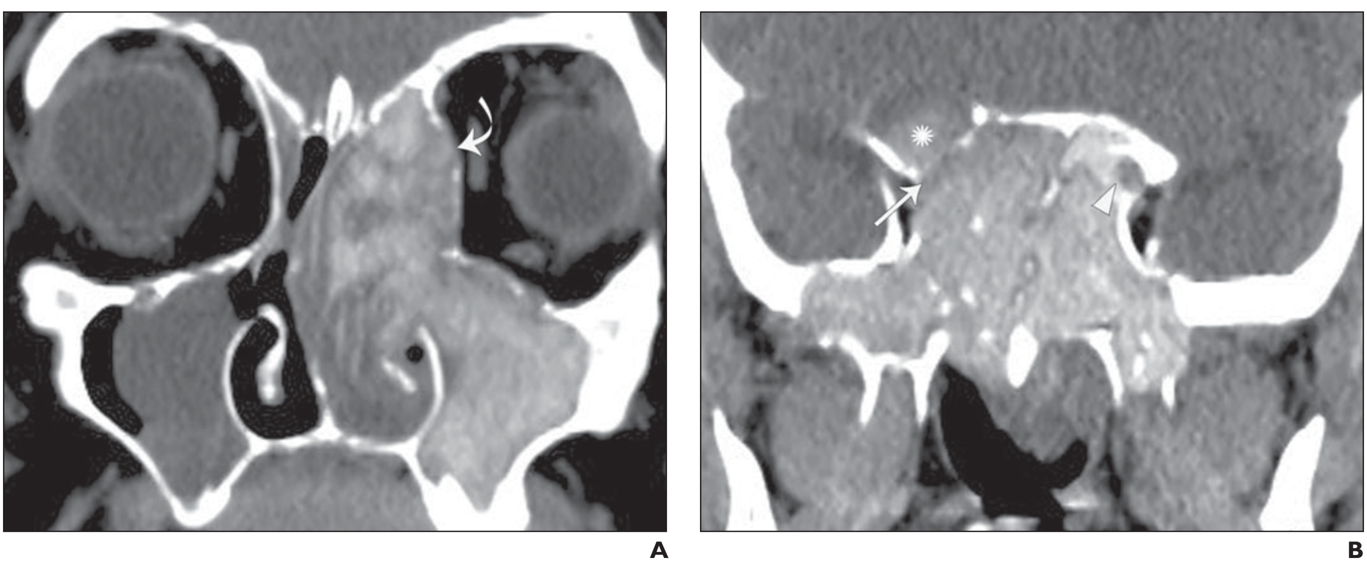

Fig. 4—17-year-old boy with allergic fungal sinusitis complicated by compression of right optic nerve. Painless decreased vision had been present in the right eye for 2 months.
A–D, Coronal (**A–C**) and axial (**D**) CT images show high-attenuation opacification of left maxillary, left ethmoidal, and bilateral sphenoidal sinuses with bone expansion and thinning. Compression of right optic nerve (*straight arrow,* **B** and **D**) is caused by expanded right anterior clinoid process (*asterisk,* **B** and **D**). Bone dehiscence is present at left lamina papyracea (*curved arrow,* **A** and **D**) and around left optic nerve (*arrowhead,* **B** and **D**), and internal carotid arteries (*arrows,* **C**). These structures are at risk of injury during functional endoscopic sinus surgery.

(Fig. 4 continues on next page)

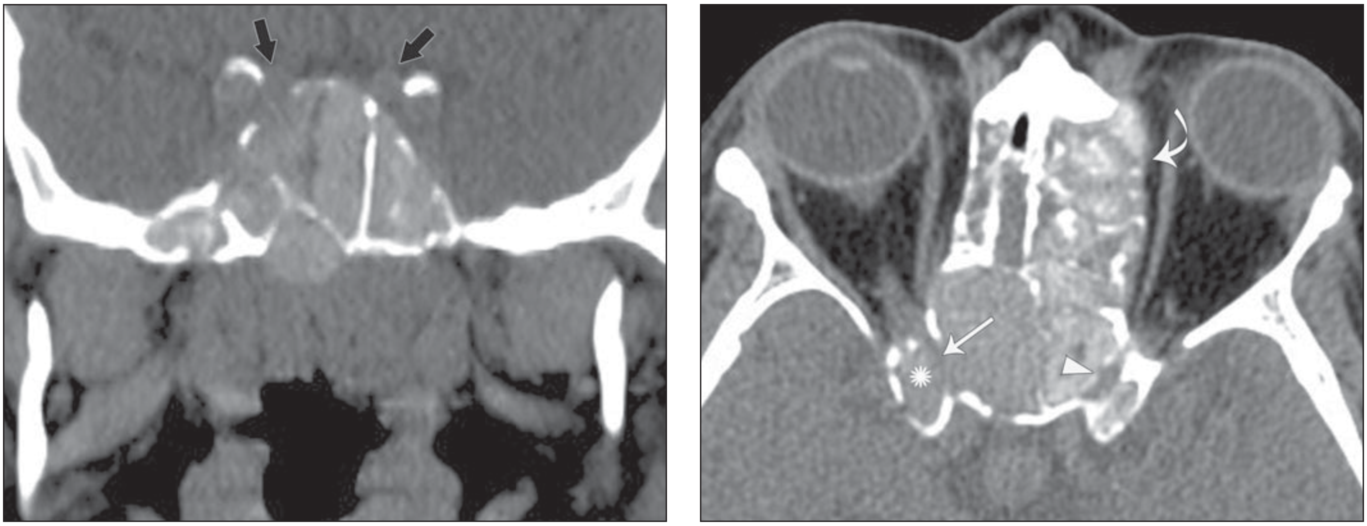

C D

Fig. 4 (continued)—17-year-old boy with allergic fungal sinusitis complicated by compression of right optic nerve. Painless decreased vision had been present in the right eye for 2 months.
A–**D,** Coronal (**A**–**C**) and axial (**D**) CT images show high-attenuation opacification of left maxillary, left ethmoidal, and bilateral sphenoidal sinuses with bone expansion and thinning. Compression of right optic nerve (*straight arrow,* **B** and **D**) is caused by expanded right anterior clinoid process (*asterisk,* **B** and **D**). Bone dehiscence is present at left lamina papyracea (*curved arrow,* **A** and **D**) and around left optic nerve (*arrowhead,* **B** and **D**), and internal carotid arteries (*arrows,* **C**). These structures are at risk of injury during functional endoscopic sinus surgery.

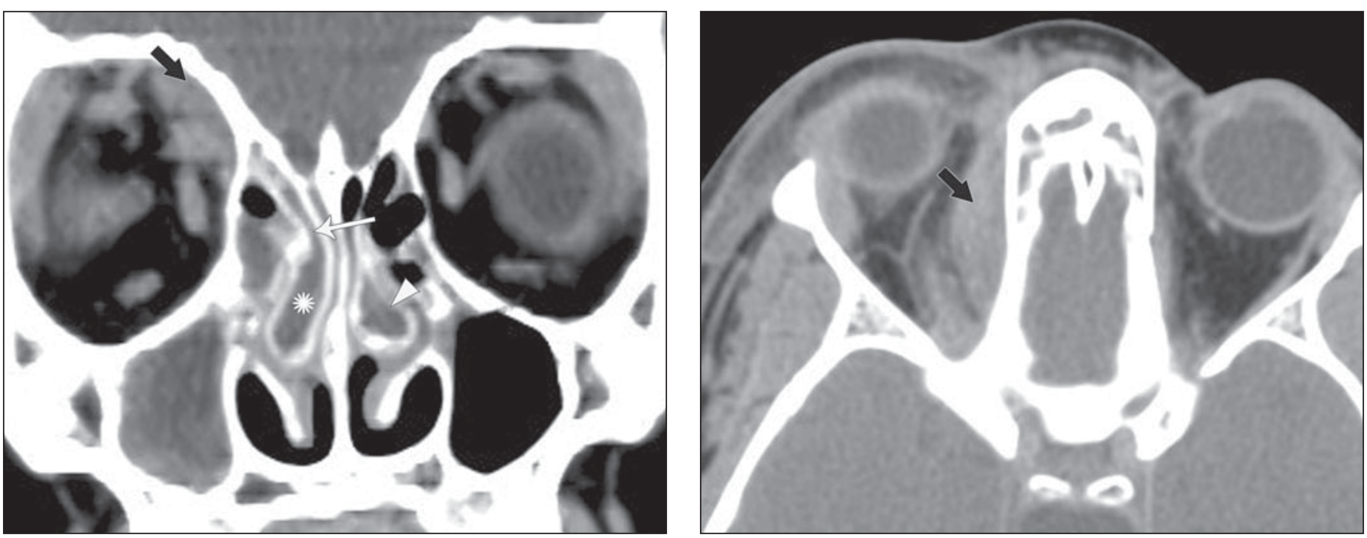

A B

Fig. 5—11-year-old girl with acute right maxillary and ethmoidal sinusitis complicated by right orbital subperiosteal abscess.
A and **B,** Coronal (**A**) and axial (**B**) CT images show opacification of right maxillary and ethmoidal sinuses. Right orbital subperiosteal abscess (*black arrow*) and overlying preseptal orbital cellulitis are present. Opacification of right concha bullosa (*asterisk,* **A**) and concha lamella (*white arrow,* **A**) was found to be pus filled at endoscopy, a finding consistent with pyocele. Left concha bullosa (*arrowhead,* **A**) also is opacified.

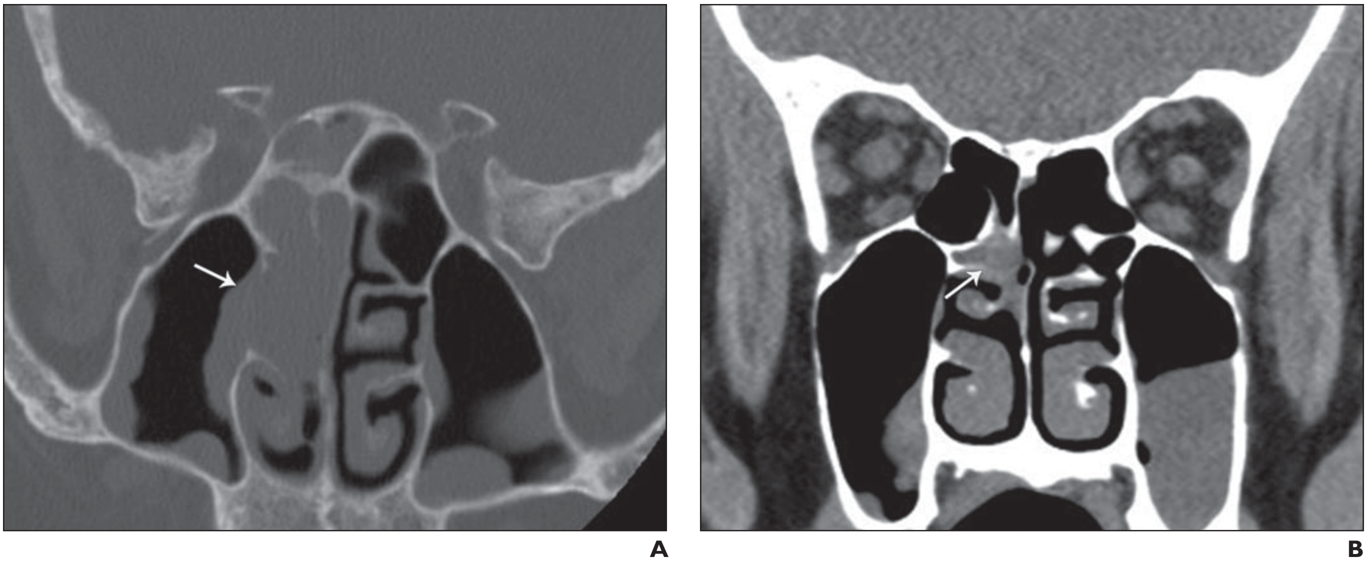

Fig. 6—82-year-old man with squamous cell carcinoma right nasal cavity mimicking nasal polyps. Manifestation was worsening right nasal obstruction.
A, Coronal CT image shows mass (*arrow*) in right nasal cavity with destruction of middle turbinate.
B, Coronal CT image shows focal opacification (*arrow*) in right nasal cavity that was present on CT image 5 months earlier but without middle turbinate destruction. Functional endoscopic sinus surgery revealed friable gritty mass.

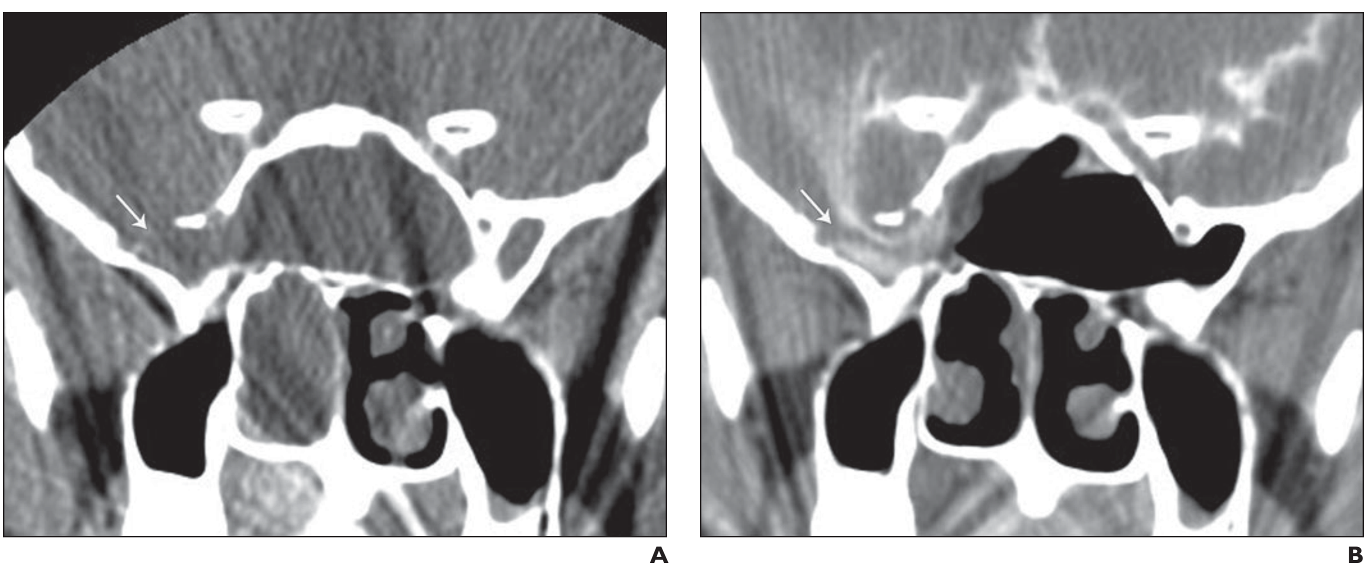

Fig. 7—50-year-old woman with CSF leak after functional endoscopic sinus surgery that was caused by preexisting cephalocele.
A, Coronal CT image obtained before surgery shows bone dehiscence in roof of opacified right sphenoidal sinus (*arrow*) and complete opacification of right nasal cavity. Functional endoscopic sinus surgery (FESS) revealed multiple polyps in right nasal cavity, posterior ethmoidal sinus, and sphenoidal sinus. Ethmoidectomy, sphenoidotomy, and polypectomy were performed.
B, Coronal CT cisternogram obtained after FESS shows CSF leak from roof of right sphenoidal sinus (*arrow*) caused by cephalocele present before FESS but not appreciated on preoperative images.

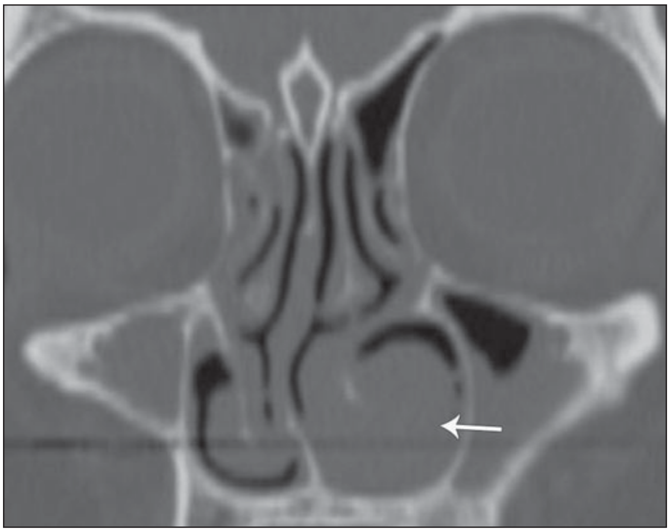

Fig. 8—43-year-old man with anomalous enlargement of inferior turbinate. Coronal CT image shows pansinus inflammatory disease and unusually large left inferior turbinate (*arrow*) that was deviating septum to right and was associated with hypoplastic left middle turbinate. Turbinate reduction procedure was performed as part of functional endoscopic sinus surgery.

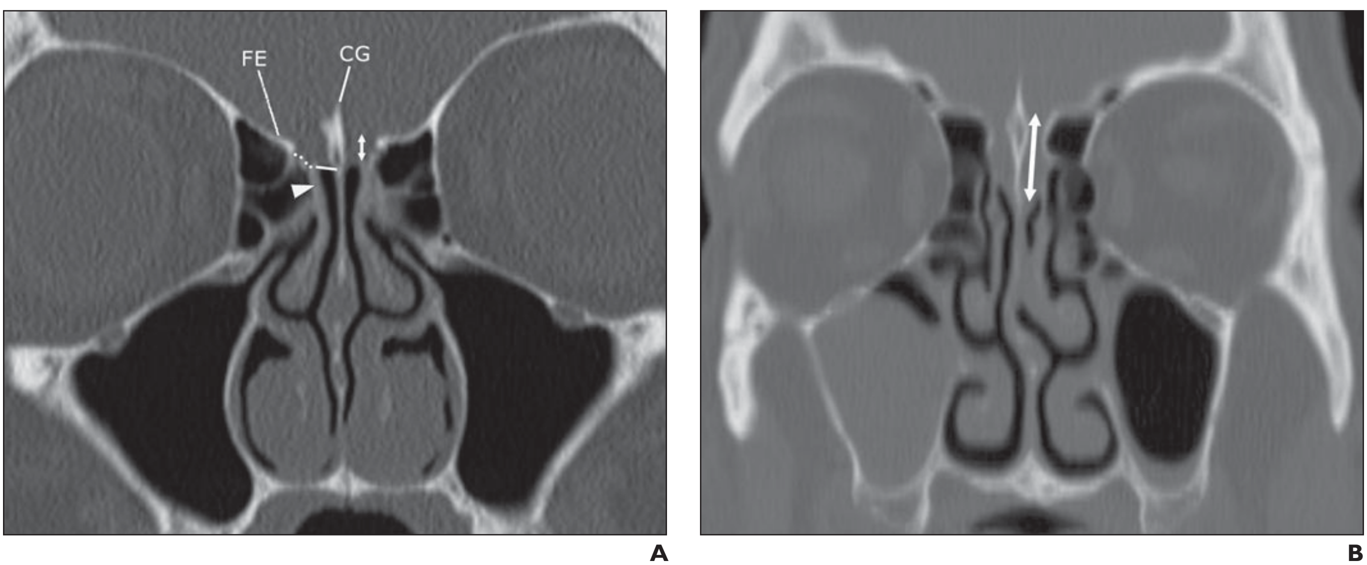

Fig. 9—Normal anatomy and critical variants in cribriform plate.

A, 34-year-old woman with normal anatomy of cribriform plate. Coronal CT image shows olfactory fossa (*double-headed arrow*) is formed by crista galli (CG) in midline, medial lamella (*white bar*) in inferior aspect, and lateral lamella (*dotted line*) in lateral aspect. Medial and lateral lamellae are separated by vertical lamella (*arrowhead*) of middle turbinate. Fovea ethmoidalis (FE) is continuation of superior orbital roof to cribriform plate. Depth of olfactory fossa (*double-headed arrow*) is less than 3 mm (Keros type 1 variant).

B, 62-year-old woman with bilateral Keros type 3 variant. Coronal CT image shows olfactory fossa is deep: distance between fovea ethmoidalis and medial lamella is greater than 7 mm (*arrow*). Keros type 2 variant is olfactory fossa depth of 3–7 mm.

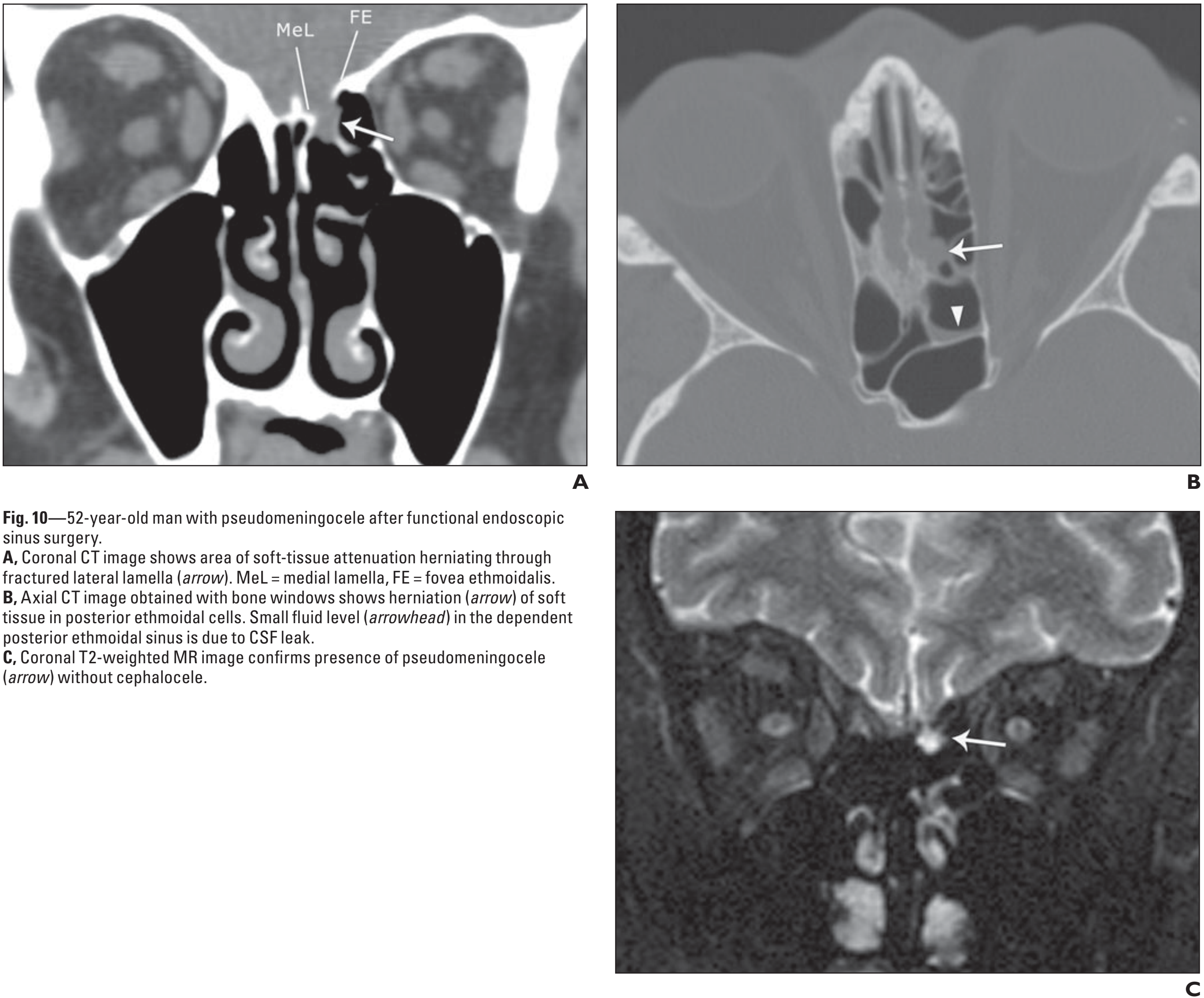

Fig. 10—52-year-old man with pseudomeningocele after functional endoscopic sinus surgery.
A, Coronal CT image shows area of soft-tissue attenuation herniating through fractured lateral lamella (*arrow*). MeL = medial lamella, FE = fovea ethmoidalis.
B, Axial CT image obtained with bone windows shows herniation (*arrow*) of soft tissue in posterior ethmoidal cells. Small fluid level (*arrowhead*) in the dependent posterior ethmoidal sinus is due to CSF leak.
C, Coronal T2-weighted MR image confirms presence of pseudomeningocele (*arrow*) without cephalocele.

Fig. 11—Anterior ethmoidal canals.
A, 42-year-old man with normal anatomy of anterior ethmoidal canals. Coronal CT image shows canals are most readily found where they form medial beak of superomedial orbital wall (*arrows*). Canal carries anterior ethmoidal artery, which is branch of ophthalmic artery, to anterior cranial fossa.
B, 55-year-old man with variant anatomy of anterior ethmoidal canals. Coronal CT image shows anomalous course of both anterior ethmoidal canals below skull base (*arrows*), making them vulnerable to injury during functional endoscopic sinus surgery.

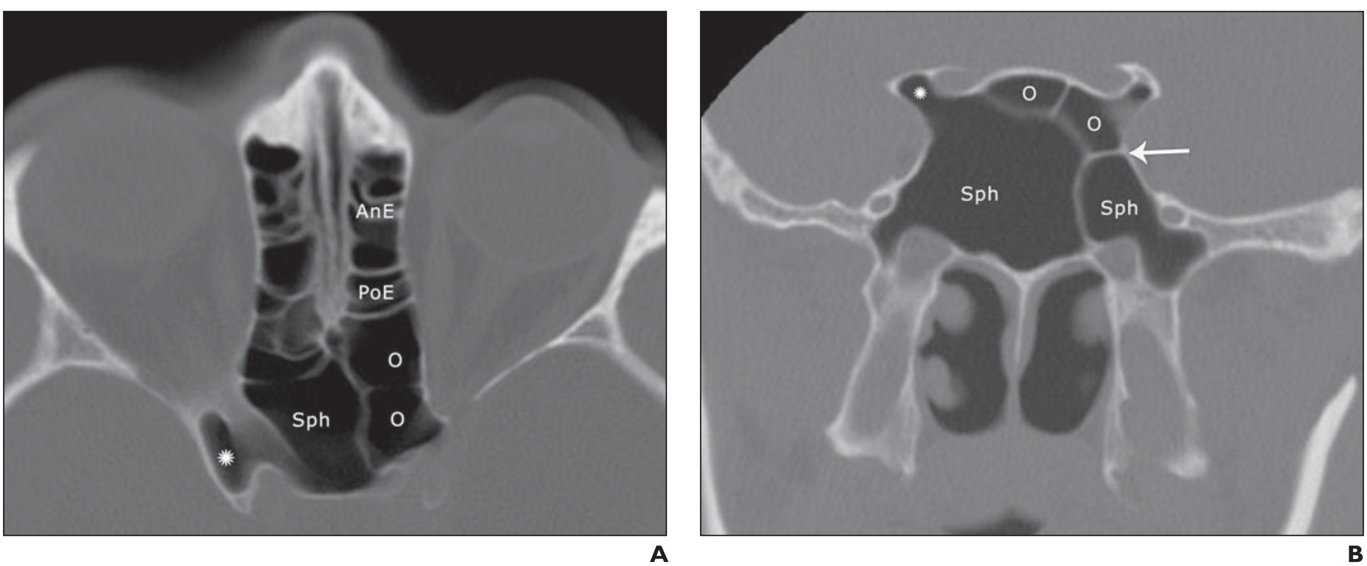

Fig. 12—43-year-old man with Onodi cells, which are defined as hyperpneumatized posterior ethmoidal air cells that extend in posterior direction above sphenoidal sinus.
A, Axial CT image shows septated air cells (O) extending into left sphenoidal sinus and anterior clinoid process (*asterisk*). AnE = anterior ethmoidal air cells, PoE = posterior ethmoidal air cells.
B, Coronal CT image shows horizontal septation (*arrow*) separating smaller left sphenoidal sinus (Sph) below from air cells (O) above. This finding is characteristic of Onodi cells. Axial and coronal images show extensive pneumatization of right sphenoidal sinus with pneumatization of anterior clinoid process (*asterisk*).

FOR YOUR INFORMATION

This article is available for CME credit. See www.arrs.org for more information.